Engineering Notes

ENGINEERING NOTES are short manuscripts describing new developments or important results of a preliminary nature. These Notes cannot exceed 6 manuscript pages and 3 figures; a page of text may be substituted for a figure and vice versa. After informal review by the editors, they may be published within a few months of the date of receipt. Style requirements are the same as for regular contributions (see inside back cover).

Helium Bubble Survey of an Opening Parachute Flowfield

Paul C. Klimas*
U.S. Naval Academy, Annapolis, Md.

Introduction

KNOWLEDGE of the flowfield surrounding a parachute, particularly during the opening, is essential to any understanding of parachute dynamics. This fundamental information, however, has yet to be satisfactorily obtained. There have apparently been no successful attempts at mapping an opening velocity field, and most of the efforts to obtain steady-state information have failed in certain regions about the canopy. The reasons for this lack of success lie with the nature of the measuring devices. They either physically obstruct the flow or opening due to their size, or cannot function in regions of high fluid rotation such as are found in wakes and mouth regions. A system which has none of these disadvantages was used by Pounder[1] in 1956 to measure steady flows about various canopies. This was done by generating helium-filled soap bubbles which were inserted into the air passing the parachute and photographed in a single plane. The neutrally buoyant bubbles were dynamically indistinguishable from the air surrounding them, and their high reflectivity made them easy to photograph. The current investigation extends the use of this concept to ascertain the velocities during a portion of the opening process. That point will be when the filling time T is unity. The nondimensional filling time is the ratio of the time measured from suspension line extension to the time interval between suspension line extension and the first attainment of a canopy projected area equal to that under steady state conditions. Two simultaneous orthogonal views of the flowfield are made, thus eliminating the need for assuming a planar flow.

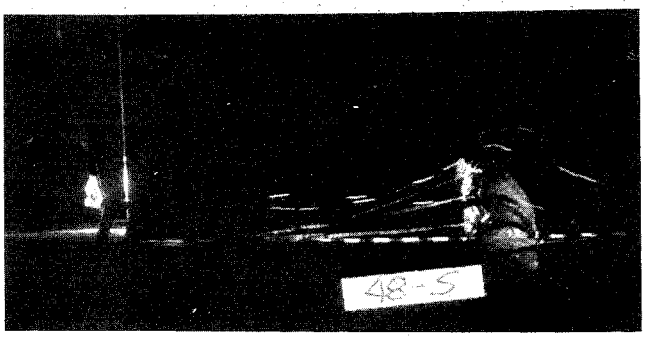

Fig. 1 Typical streak photograph (side view) at $T = 1$.

Received January 30, 1973. This work was supported by the U.S. Army Airdrop Engineering Laboratory, Natick, Massachusetts.

Index categories: Entry Deceleration Systems and Flight Mechanics (e.g., Parachutes); Nonsteady Aerodynamics; Aircraft Deceleration Systems.

*Assistant Professor, Aerospace Engineering Department. Associate Member AIAA.

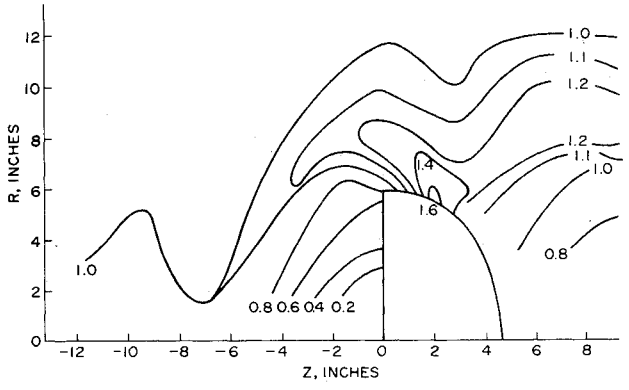

Fig. 2 Contours of constant axial velocity ratio, $Vz/V\infty$, at $T = 1$.

Apparatus

The investigation was conducted in the United States Naval Academy $3\frac{1}{2} \times 4\frac{1}{2}$ ft subsonic wind tunnel. The particular parachute model used was an 18 gore, 18 in. nominal diameter flat circular type having a 1.8-in.-diam vent. Tunnel blockage limited the nominal diameter to this value. The model was constructed of 1.1 oz rip-stop nylon, MIL-C-7020, Type I, having a permeability of 114 $ft^3/ft^2/min$. The suspension lines were 18 in. long and were tied to a $\frac{15}{16}$-in.-diam steel ring. The model deployment system consisted of a 3-in.-diam, 12-in. long streamlined aluminum tube mounted along the tunnel centerline into which the parachute was loosely packed. Deployment was initiated by raising a solenoid driven pin which allowed a dead-fall weight to extract the parachute from the tube. The model then rode along a 5 ft. long, 0.25-in.-diam aluminum rod to a point where the moving stream began the inflation. The rod served the dual purposes of stabilizing the motion and, since it was graduated into 1-in. intervals, of providing a length scale. In steady operation the suspension line ring was located some 6 in. downstream of the deployment tube.

The flow visualization itself centered around a Sage Action, Inc. bubble generating system. The density of each

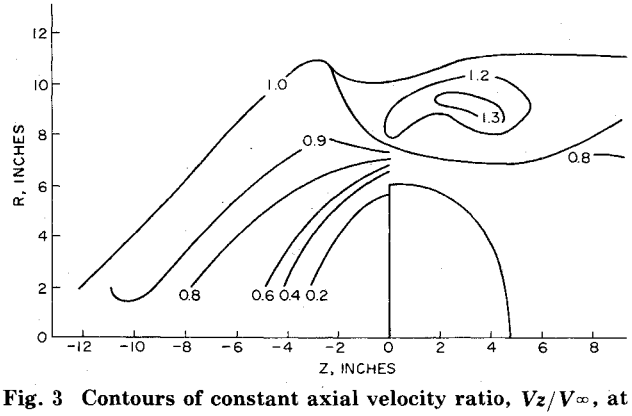

Fig. 3 Contours of constant axial velocity ratio, $Vz/V\infty$, at $T = \infty$.

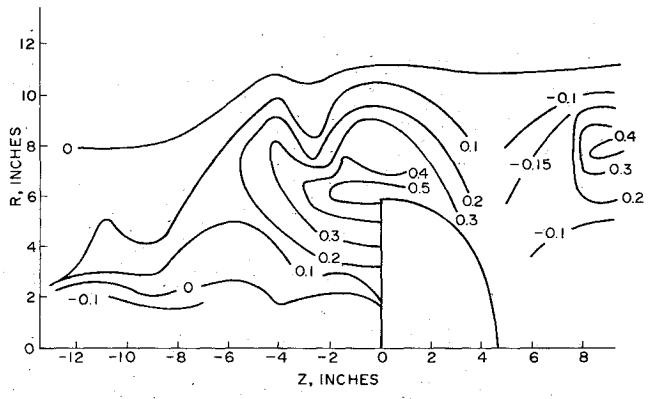

Fig. 4 Contours of constant radial velocity ratio, $Vr/V\infty$, at $T = 1$.

bubble was reportedly within 2% of the air value. Simultaneous photographs were taken by two still cameras mounted at right angles to each other and located 72 in. off the tunnel centerline. ASA 3000 speed film was used and illumination was provided by a high intensity Xenon arc lamp mounted 8 ft upstream of the center of the test section and somewhat off axis. Although this presented the possibility of some disturbance to the freestream, it was necessary to sufficiently illuminate the upstream flow.

Experiment

The original experimental plan was to take a large number of photographs at each of four or five different fractions of the filling time. Each set of photographs would include a number of randomly placed streaks. This would provide a description of the particle velocities over the full range of opening times. However, it was found that in order to get well defined streak photographs, the bubble residence time needed to be that corresponding to a freestream velocity of approximately 10 fps. Horizontal parachute operation, particularly during opening, at these speeds gave a ratio of aerodynamic to static forces which rendered the opening asymmetrical. It wasn't until the process had progressed to $T \approx 1$ that the lack of symmetry became small enough to be considered negligible. For these times and those beyond, the differences in the maximum radii between the upper and lower portions of the canopy were less than 7% of the average of these two extremes. Future studies should either take place in a vertical wind tunnel or combine greater levels of illumination with increased airspeeds.

The tunnel speed was set at 8.5 fps. A series of streak photographs taken with the model undeployed gave a tunnel axial velocity of 8.36 fps, a radial velocity of 0.26 fps, and a circumferential velocity of 0.51 fps. Errors of the magnitude of the last two values would be expected in locating streaks made by the 0.125-in.-diam bubbles and exposure time used here.

The actual opening time was found to be 0.82 sec by taking photographs at various time intervals measured from initiation of deployment. The cameras taking the simultaneous photographs were synchronized by electronic time delay and each set to a 0.0117 ± 0.0005 sec exposure time. Ambient pressure and temperature for the tests were 30.53 in Hg and 90°F, respectively.

Approximately 25 pairs of photographs were taken at both $T = 1$ and in steady state. The bubble generating head was mounted at various radial locations in order to sufficiently cover the field. This resulted in roughly 250 matchable streaks for each of the two cases. A typical side view photograph is shown in Fig. 1. This is an unsteady shot, as may be seen by the whipping action of some of the suspension lines. The generating head is resting on the deployment tube.

Results

The basic results of the study are given in Figs. 2–5. These map lines of constant nondimensional axial and radial velocity as functions of flowfield location. This information was obtained from each pair of photographs considering the fact that each camera had a conical field of view with a 72 in. altitude. Axial locations of each streak from top and side views usually agreed within ¼ in. Circumferential velocities were typically less than ±0.5–0.7 fps. Consequently, the velocities are considered to be functions of axial and radial location only. The particles were generally found in a 30°–35° sector centered about the radial along which they were inserted. This scatter substantiated the postulated necessity of taking the two orthogonal views.

One of the two salient points of contrast between the unsteady and steady flowfields are the relative dimensions of the turbulent regions. These regions are shown as being void of data. The large area of turbulence near the mouth previously seen by Lockman[2] in his pressure rake survey is certainly in evidence in the steady-state data but nonexistent in the opening model. The wake sizes also differ. The average vent plane area of the steady wake is roughly 2.4 times the corresponding value for the $T = 1$ case. Secondly, it can be seen that the effects of the opening canopy are confined to regions relatively close to it, while those of the steadily operating parachute extend much further. The lack of data over the first one or two inches of radius is due to the fact that the generating head could not be placed any closer to the centerline than 1½ in. without obstructing the opening or being set into the parachute rigging lines.

The aberrations seen between 10 and 14 in. upstream are due to the suspension lines and ring. Here, due to the relatively high density of 18 looped lines, there is an obstacle to the flow.

A few qualitative observations were made while optically viewing the steady-state condition. In the regions of turbulence and those bordering them, the bubbles oscillate. This vibratory motion is superposed upon any other motion. Motions characteristic of ring vortices parallel to the mouth plane and trailing vortices were also observed in the wake. The highly irregular nature of this flow would require considerably more data than that collected here to get any direct measurement of net average velocities in this region. A reasonable value could, however, be obtained by applying the conservation of mass to the region using the known velocity distributions in the nonturbulent

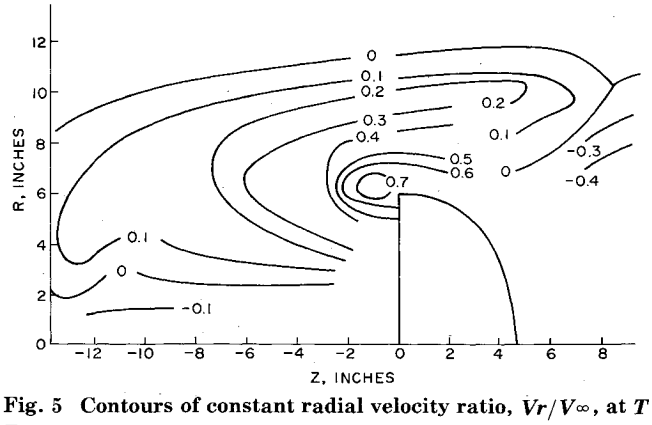

Fig. 5 Contours of constant radial velocity ratio, $Vr/V\infty$, at $T = \infty$.

portions of the flow. Doing this here gives uncharted vent plane region velocities of $-0.49V\infty$ and $+0.65V\infty$ for the unsteady and steady cases, respectively. Considering the rapidly expanding canopy, the reverse flow in the unsteady case is not at all unreasonable. It is a well known fact that at $T = 1$ the canopy is being compressed in the axial direction.

Concluding Remarks

The velocity profiles about a flat circular parachute model have been found for both a time late in the inflation process when the canopy shape is close to the steady-state value and in steady-state. The previous unavailability of any similar data for the former case makes it quite useful for assessing any analytical attempts at describing the kinetics of opening. The data also suggest that the extent of the flow which is turbulent during opening is probably small enough that a potential flow mathematical model would give a reasonable description of the opening process.

References

[1]Pounder, E., "Parachute Inflation Process Wind-Tunnel Study," WADC TR 56-391, Sept. 1956, Equipment Laboratory, Wright-Patterson Air Force Base, Ohio, pp. 17–18.

[2]Lockman, W. K., "Analysis of an Inflating Subsonic Reefed Parachute with Experimental Mass Flow Study," MS thesis, Nov. 1963, Univ. of Minnesota, Minneapolis, Minn., pp. 119–141.

Experimental Study on Optimization Parameters of a Supersonic Jet Ejector Thrust Augmentor

Dah Yu Cheng* and Peter Wang†
University of Santa Clara, Santa Clara, Calif.
and
Dean M. Chisel‡
NASA Ames Research Center, Moffett Field, Calif.

Introduction

THE present experimental data were aimed at obtaining the effect of jet mixing, the effective length/diameter of the ejector tube, the entrance length shape factor, the shape loading, and the optimum primary jet location. The most effective thrust weight of the ejector tube was also examined from airborne vehicle point of view.

Simplified Theory

The similarity velocity profiles of a turbulent jet issuing from a wall was first analyzed by Schlichting.[1] The streamlines were shown in Fig. 1a. The velocity profiles

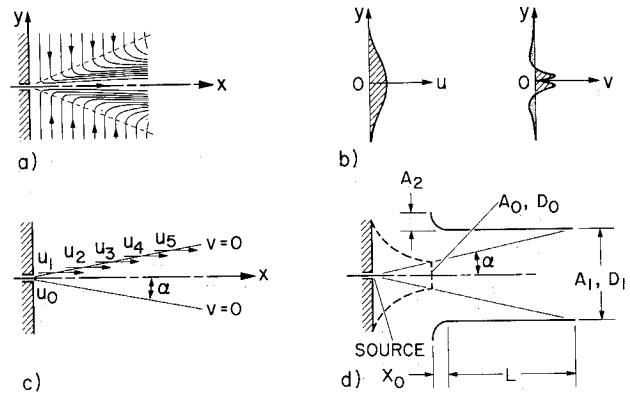

Fig. 1 a) Streamlines of a circular wall jet. b) The velocity profiles u, v, as a function of y at an arbitrary x location. c) $v = 0$ line, and the induced velocity. d) Parameters of a jet agumentor experiment.

have similarity solutions given as

$$u = \frac{3}{8\pi}\frac{K}{\epsilon_0 x}\frac{1}{(1 + 1/4\eta^2)^2};$$

$$v = \frac{1}{4}\left(\frac{3}{\pi}\right)^{1/2}\frac{(K)^{1/2}}{x}\frac{[\eta - (1/4)\eta^2]}{[1 + (1/4)\eta^2]^2}$$

where

$$\eta = \frac{1}{4}\left(\frac{3}{\pi}\right)^{1/2}\frac{(K)^{1/2}}{\epsilon_0}\frac{y}{x};\quad K = 2\pi\int_0^\infty u^2 y dy$$

ϵ_0 is the turbulent kinematic viscosity. In subsonic flow $\epsilon_0/(K)^{1/2}$ was found to be a constant[2]; therefore, variation of jet momentum K does not change the geometrical pattern of the streamline with respect to y, and x. The velocity profile of the radial component v has a zero point (Fig. 1b) due to the expansion of the streamlines in the center region just compensated by the induced inward velocity. This occurs at $\eta = 2$. The velocity crossing $\eta = 2$ line has u component only and it is a measure of the induction mass. From experimental data of Riechardt[2] $\epsilon_0/(K)^{1/2} = 0.0161$, hence $\eta = 2$ line has an angle of $\alpha = 7.5°$ (Fig. 1c). If an ejector is added to a jet, from the above streamline analysis apparently the ejector length beyond the interception point of $(v = 0)$ line contributes nothing to the ejector pumping action; therefore, the ejector only requires a fixed L/D according to α regardless of their diameter.

A finite diameter jet for the real experimental case can be simulated by a jet source at an appropriate location in-

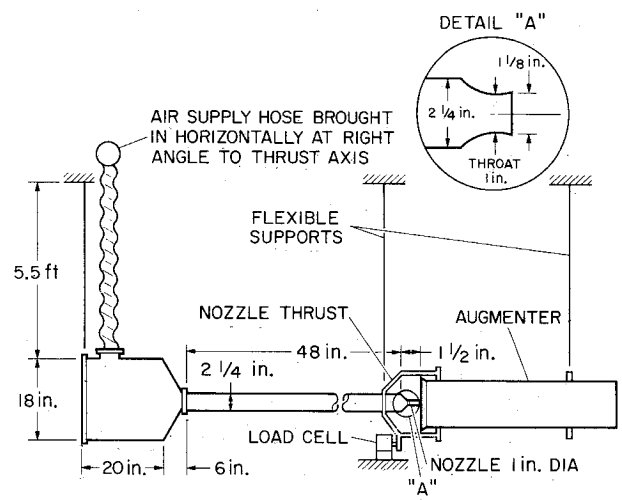

Fig. 2 The test setup.

Received January 26, 1973; revision received April 27, 1973. This work is partially supported by NASA-University Grant NGR-05-017-033.

Index categories: Aircraft Noise, Powerplant; Jets, Wakes, and Viscid-Inviscid Flow Interaction; Airbreathing Engine Testing.

*Senior Research Associate, Mechanical Engineering Department. Member AIAA.

†Research Assistant.

‡Research Scientist.